Marine Biology (2004) 144: 633–640
DOI 10.1007/s00227-003-1226-1

RESEARCH ARTICLE

R. Hill · U. Schreiber · R. Gademann
A. W. D. Larkum · M. Kühl · P. J. Ralph

Spatial heterogeneity of photosynthesis and the effect of temperature-induced bleaching conditions in three species of corals

Received: 24 June 2003 / Accepted: 18 September 2003 / Published online: 16 January 2004

Abstract Heterogeneity in photosynthetic performance between polyp and coenosarc tissue in corals was shown using a new variable fluorescence imaging system (Imaging-PAM) with three species of coral, *Acropora nobilis*, *Cyphastrea serailia* and *Pocillopora damicornis*. In comparison to earlier studies with fibre-optic microprobes for fluorescence analysis, the Imaging-PAM enables greater accuracy by allowing different tissues to be better defined and by providing many more data points within a given time. Spatial variability of photosynthetic performance from the tip to the distal parts was revealed in one species of branching coral, *A. nobilis*. The effect of bleaching conditions (33°C vs. 27°C) was studied over a period of 8 h. Marked changes in fluorescence parameters were observed for all three species. Although a decline in Φ_{PSII} (effective quantum yield) and Yi (the first effective quantum yield obtained from a rapid light curve) were observed, *P. damicornis* showed no visual signs of bleaching on the Imaging-PAM after this time. In *A. nobilis* and *C. serailia*, visual signs of bleaching over the 8 h period were accompanied by marked changes in F (light-adapted fluorescence yield), NPQ (non-photochemical quenching) and E_k (minimum saturating irradiance), as well as Φ_{PSII} and Yi. These changes were most marked over the first 5 h. The most sensitive species was *A. nobilis*, which after 8 h at 33°C had reached a Φ_{PSII} value of almost zero across its whole surface. Differential bleaching responses between polyps and coenosarc tissue were found in *P. damicornis*, but not in *A. nobilis* and *C. serailia*. NPQ increased with exposure time to 33°C in both the latter species, accompanied by a decreasing E_k, suggesting that the xanthophyll cycle is entrained as a mechanism for reducing the effects of the bleaching conditions.

Communicated by L. Hagerman, Helsingør

R. Hill · P. J. Ralph (✉)
Institute for Water and Environmental Resource Management and Department of Environmental Sciences,
University of Technology, Westbourne St Gore Hill,
2065 Sydney, NSW, Australia
E-mail: Peter.Ralph@uts.edu.au
Tel.: +61-2-95144070
Fax: +61-2-95144003

U. Schreiber
Julius-von-Sachs Institut für Biowissenschaften,
Universität Würzburg, Würzburg, Germany

R. Gademann
Gademann Meßtechnik, Dürrbachtal, Würzburg, Germany

A. W. D. Larkum
School of Biological Sciences, University of Sydney,
2006 Sydney, NSW, Australia

M. Kühl
Marine Biological Laboratory, University of Copenhagen,
Strandpromenaden 5, 3000 Helsingør, Denmark

Introduction

Reef-forming corals consist of a symbiotic association between a cnidarian host and unicellular symbiotic dinoflagellates, known as zooxanthellae. The zooxanthellae provide photosynthate to support the host's metabolic processes. Coral bleaching is characterised by the loss of zooxanthellae from the coral or a decrease in chlorophyll concentration inside coral tissue (Hoegh-Guldberg and Smith 1989; Szmant and Gassman 1990; Fitt et al. 1993). The primary cause of bleaching is thought to be linked to dysfunction of photosystem II (PSII) (Warner et al. 1996) or of the Ci uptake system in zooxanthellae (Jones et al. 1998). The signal triggering expulsion of zooxanthellae from the host is not known. The breakdown of the symbiosis between the hermatypic coral host and zooxanthellae can, in severe cases, result in the death of the coral, which can lead to widespread degradation of coral reefs (Hoegh-Guldberg 1999). Corals are highly susceptible to extreme environmental conditions (Marshall and Baird 2000) and anthropogenic impacts (Jones and Hoegh-Guldberg 1999; Ravindran et al. 1999; Bruno et al. 2001). Combined high temperatures and intense light have been identified as

major causes of coral bleaching (Cook et al. 1990; Fitt et al. 2001; Yentsch et al. 2002). Knowledge of the physiological processes that accompany bleaching is needed for a clear understanding of the mechanisms of coral bleaching.

Corals often show a heterogeneous distribution of photosynthetic activity (Kühl et al. 1995; Rowan and Knowlton 1995; Helmuth et al. 1997), e.g. a variation in photosynthetic light acclimation between the polyp tissue and the coenosarc tissue in-between polyps (Ralph et al. 2002). The detection of spatial heterogeneity in variable chlorophyll *a* (chl *a*) fluorescence parameters gives a direct indication of the variation in physiological processes operating across a heterogeneous photosynthetic surface. The newly developed Imaging-PAM (Walz, Effeltrich, Germany) allows investigation of photosynthetic surfaces (up to 20×30 mm), by capturing two-dimensional images of chl *a* fluorescence yields. With this system, spatial variations can now be examined at scales of < 0.5 mm within a single image, whereas previously measurements were limited to either integral measurements from 2 to 8 mm wide areas with a Diving-PAM or, alternatively, a moderate number of microscale measurements with a Microfibre-PAM system (both used by Ralph et al. 2002). Variations in stress-induced changes across a coral can now be identified and related to structures that are more susceptible to damage and/or down-regulation of photosynthesis. The Imaging-PAM is therefore a very powerful new tool for assessing spatial and temporal changes occurring in the photosynthetic apparatus of zooxanthellae when the coral host is exposed to bleaching conditions.

In the present paper the potential for using the Imaging-PAM to identify spatial heterogeneity in branching and massive corals was compared with previous methods using the Microfibre-PAM. In addition, the effects of bleaching conditions (33°C for up to 8 h) were examined, by assessing F (light-adapted fluorescence), $rETR_{max}$ (maximum observed relative electron transport rate), Φ_{PSII} (effective quantum yield), Yi (the first effective quantum yield obtained from a rapid light curve), NPQ (non-photochemical quenching) and E_k (minimum saturating irradiance), and comparing changes in polyp and coenosarc tissue.

Materials and methods

Coral specimens

Upper branches of sun-adapted colonies of three species of coral, *Pocillopora damicornis* (Linnaeus), *Acropora nobilis* (Dana) and *Cyphastrea serailia* (Forskål), were collected from the outer reef lagoon flat of Heron Island (152°06′E; 20°29′S) between 26 January and 4 February 2003. Corals were maintained under shaded conditions (< 200 μmol quanta m^{-2} s^{-1}) at 27°C prior to the experiment (ambient lagoon temperature). Bleaching treatments were applied for up to 8 h (33°C and 280 μmol quanta m^{-2} s^{-1}) with actinic light provided by a halogen lamp (12 V, 150 W with a UV-blocking filter). Each sample was placed in a separate flow-through chamber (2.8 l; Fig. 1), where water temperature inside the chamber was maintained using a temperature-regulated water bath (Julabo Labortechnik F20-MH Seelbach, Germany).

Fluorescence measurements

The Imaging-PAM (Walz, Effeltrich, Germany) was designed for mapping heterogeneity in photosynthetic activity by examining the two-dimensional distribution of chl *a* fluorescence from photosynthetic tissues. We used the submersible Imaging-PAM system to measure the light-adapted fluorescence yield (F) and maximum light-adapted fluorescence yield (F_m'). Since no widely accepted absorption coefficients have yet been developed for corals, the relative electron transport rate (rETR) was calculated as $rETR = \Phi_{PSII} \times PAR$, where $\Phi_{PSII} = (F_m' - F)/F_m'$. The rETR measurements were obtained through the application of a series of saturation pulses under increasing actinic irradiance (0, 31, 81, 120,

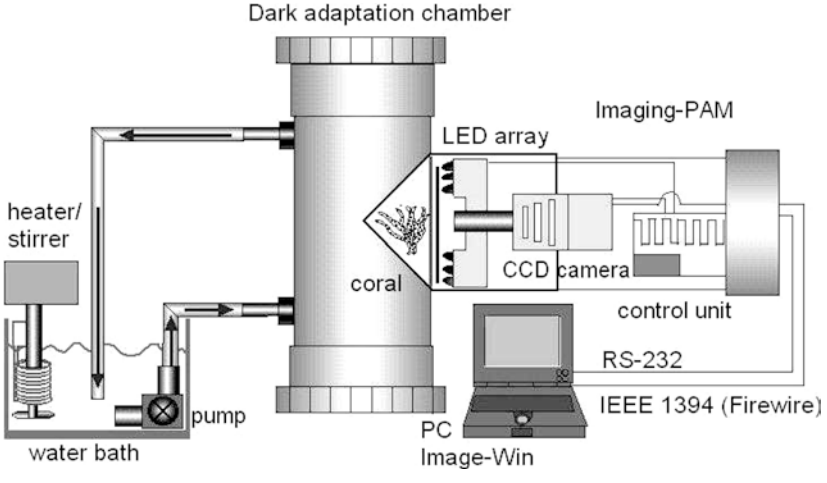

Fig. 1 Experimental set-up, showing a coral sample inside the dark-adaptation chamber. The water is circulated by a pump and kept at the required temperature using a heater stirrer. The Imaging-PAM comprises a CCD camera, LED array and control unit that synchronises the LEDs and image capture. The CCD camera captures the fluorescence emission from the coral, while the RS232 and IEEE 1394 firewire cables allow for communication and image transfer between the image control unit and personal computer. The LED array applies the blue excitation light (470 nm)

185, 295, 385, 480, 610, 770 and 975 μmol quanta m^{-2} s^{-1}) in the form of a rapid light curve (RLC; Ralph et al. 2001). The RLC measurements utilised a Φ_{PSII} determination at the end of a 10 s period at each irradiance level. The first effective quantum yield (Φ_{PSII}) obtained from a RLC (Ø μmol quanta m^{-2} s^{-1}) measured during the pseudo-dark period before the curve commences is termed Yi. The non-photochemical quenching [$NPQ = (F_m - F_m')/F_m'$] was determined as the highest NPQ value on the RLC. To quantitatively compare several descriptive parameters (α, E_k and $rETR_{max}$) of the measured RLCs, a double exponential decay function (Platt et al. 1980) was fitted to the empirical data using Sigmaplot 2001 (v7.0, SPSS) (for further details see Kühl and Revsbech 2001; Ralph et al. 2002) such that:

$$P = P_s\left(1 - e^{-(\alpha E_d/P_s)}\right)e^{-(\beta E_d/P_s)} \quad (1)$$

In the absence of photoinhibition ($\beta = 0$), the function becomes a standard rectangular hyperbola, with an asymptotic maximum rETR value (Harrison and Platt 1986), and Eq. 1 can be simplified to:

$$P = P_m\left(1 - e^{-(\alpha E_d/P_m)}\right) \quad (2)$$

Here P_s is a scaling factor defined as the maximum potential rETR in the absence of photoinhibitory processes, P_m is the photosynthetic capacity at saturating irradiance, α is the initial slope of the RLC before the onset of saturation, E_d is the downwelling irradiance (400–700 nm) and β characterises the slope of the RLC beyond the onset of photoinhibition. The parameters $rETR_{max}$ and E_k were estimated using the following equations:

$$rETR_{max} = P_s[\alpha/(\alpha+\beta)]/[\beta/(\alpha+\beta)]^{\beta/\alpha} \quad (3)$$

and

$$E_k = rETR_{max}/\alpha \quad (4)$$

Experimental protocol

Four replicate corals of each species exposed to the control conditions, i.e. 280 μmol quanta m^{-2} s^{-1} and 27°C, were measured by the Imaging-PAM to obtain PAR absorptivity, F, F_m' and rETR data. Over a period of an hour, the water temperature was then raised to 33°C, while the light remained at 280 μmol quanta m^{-2} s^{-1}. After 1 h at 33°C and 280 μmol quanta m^{-2} s^{-1}, the Imaging-PAM measurements were taken. Imaging-PAM measurements were taken every hour for 8 h. From the data collected, independent values for the polyp and coenosarc structures were calculated. For each individual replicate, polyp and coenosarc values were obtained by averaging three polyp and three coenosarc regions defined as independent "areas of interest" (AOI) with the Imaging-PAM software. This was performed for each of the four replicate corals.

Statistical analysis

Variation in F and F_m' measurements for the polyp and coenosarc were tested using a repeated measures one-way analysis of variance model (rmANOVA, $\alpha = 0.05$). In these situations the assumptions of normality and equal variance were satisfied, thus allowing for the use of a parametric analysis. For the rETR ($rETR_{max}$ and E_k) and the Yi measurements these assumptions were not always satisfied. When normality and equal variance were not achieved, the non-parametric Kruskal–Wallis test was performed to assess variation between the treatments. These analyses were performed using Minitab Statistical Software 13.1 (vers. 2000). In order to determine if significant differences existed between the polyp and coenosarc regions, the sign test was applied (Lewis 1966).

Results

Bleaching conditions of 33°C and 280 μmol quanta m^{-2} s^{-1} were applied to the three coral species studied and observations were made over a period of 8 h. The ongoing fluorescence yield (F) images obtained at each temperature treatment for two species, *Acropora nobilis* and *Cyphastrea serailia*, are shown in Fig. 2 (results for *Pocillopora damicornis* indicated a lack of bleaching and are not shown). These time-series images represent a single replicate, but from each image a given number of points can be chosen for assessing the effect of temperature over the time period (and these are shown in Fig. 3). The images give detailed insight into the heterogeneity occurring between the polyp and coenosarc regions of the corals, where the polyps had a greater fluorescence yield (F) than the coenosarc. With increasing length of exposure to the bleaching temperature of 33°C, some changes across the coral surface were observed. *P. damicornis* showed the least variation when compared across treatments, whereas *A. nobilis* and *C. serailia* showed a clear gradient with increasing exposure time to 33°C, and the fluorescence emissions declined with each successive treatment (Fig. 2). A longitudinal gradient is clearly evident in the images for *A. nobilis*, with the tip region showing less fluorescence than the distal regions especially with the onset of bleaching. In contrast, the massive *C. serailia* showed less evident spatial heterogeneity, apart from the polyp/coenosarc distinction, although even here it is clear that some regions are reacting differently to others.

The greatest change in Φ_{PSII} was seen in *A. nobilis*, where it reached zero across most of the sample area after the 8 h treatment (Fig. 2). By comparison, *C. serailia* (Fig. 2) and *P. damicornis* (not shown) had a much smaller, but significant (see Yi in Table 1), decline in Φ_{PSII} with increasing length of exposure to 33°C. The Φ_{PSII} images presented in Fig. 2 show very little heterogeneity across the coral surfaces, whereas variation was expected between the polyp and coenosarc regions. However, the F and F_m' values varied equally in amplitude at each temperature treatment, as seen in Fig. 3a–c, therefore Φ_{PSII} values were similar.

Values of F, F_m' and NPQ for *A. nobilis* showed a significant decline in F (39% decline in the polyps and 43% decline in the coenosarc) from the control temperature (27°C) to the 33°C/1 h treatment (Fig. 3b), and then remained relatively constant. The polyp and the coenosarc both followed similar trends; however, the coenosarc values were significantly lower than those of the polyp (sign test $P < 0.05$). In *C. serailia*, the F values of both the polyp and coenosarc gradually decreased over 5 h, to 45% in the polyp and 42% in the coenosarc (Fig. 3c). After 5 h at 33°C, F remained constant. The F readings from the polyp and coenosarc of this species showed very similar trends over the different temperature treatments; however, the F values of the polyp were greater than those of the coenosarc (sign test).

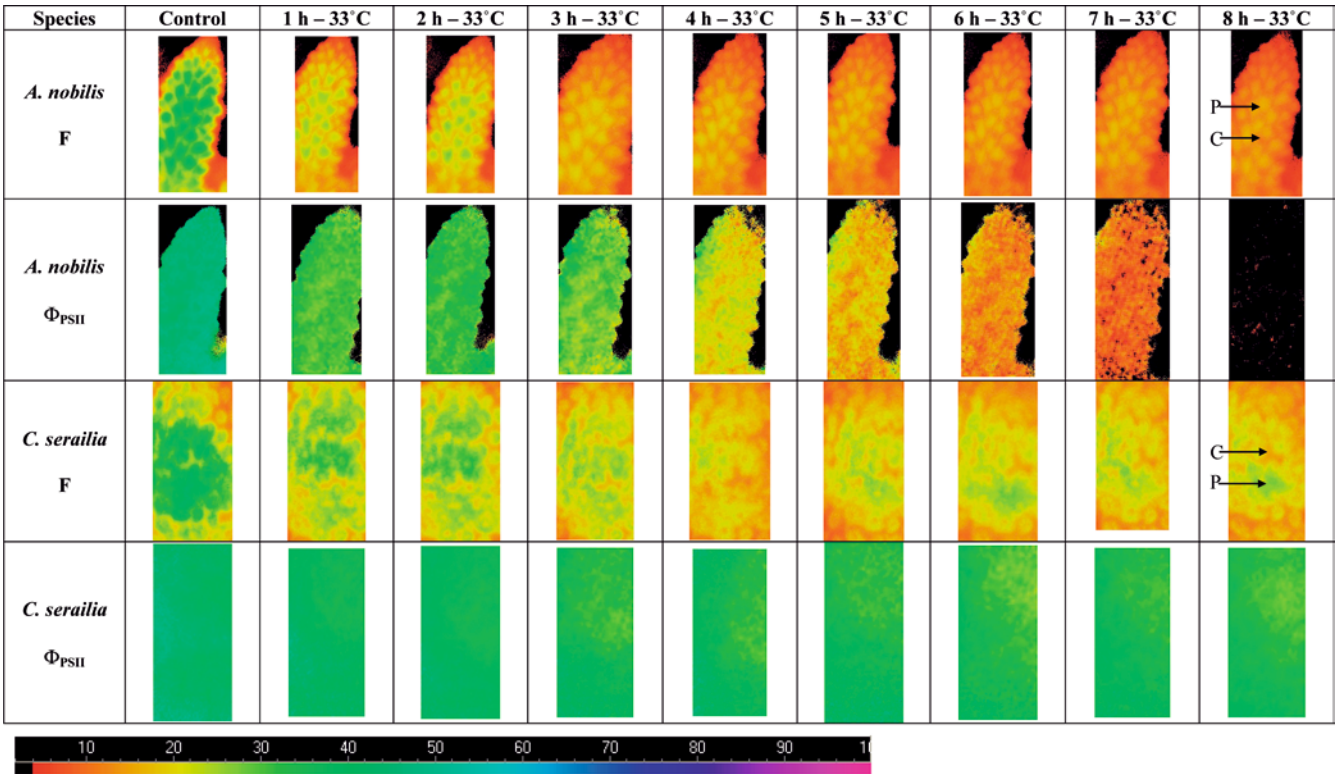

Fig. 2 *Acropora nobilis*, *Cyphastrea serailia*. Representative images of the base fluorescence (F) and effective quantum yield (Φ_{PSII}) for the control (27°C) and 33°C/1–8 h treatments (one of four replicates shown). These images show the spatial heterogeneity and are representative of the four replicates. Base length of images is ~8 mm. The *colour gradient scale* indicates the magnitude of the fluorescence signal represented by each colour. On the 8 h F images the polyp (P) and coenosarc (C) tissues are indicated

For both *A. nobilis* and *C. serailia* the F_m' values declined more strongly than for F over the first 5 h (22% decline in the polyps and 21% decline in the coenosarc in *A. nobilis* and 40% decline in the polyps and 41% decline in the coenosarc in *C. serailia*). After 5 h, both species continued to decrease in F_m', at a much slower rate. This trend was observed in both the polyp and coenosarc; however, once again, the values from the coenosarc were significantly lower (Fig. 3b, c).

In contrast, *P. damicornis* showed a fairly constant F for each temperature treatment (Fig. 3a); however, the F of the coenosarc was found to be significantly lower than that of the polyp (sign test $P < 0.05$). F_m' values for the polyp and coenosarc of *P. damicornis* showed similar trends over the nine temperature treatments, where the coenosarc showed a significantly lower F_m' for each treatment as determined by the sign test ($P < 0.05$). F_m' values remained constant from the control temperature to the 33°C/2 h treatment, after which it began to decline.

Non-photochemical quenching

The amount of NPQ dissipated by each species in each temperature treatment is illustrated in Fig. 3d–f. In *A. nobilis*, a significant increase in NPQ occurred as the length of exposure to 33°C increased (Fig. 3e). The sign test indicated that the polyp had a greater NPQ than did the coenosarc tissue at all time points except 4 and 6 h. *C. serailia* showed a gradual increase in NPQ with increasing time at 33°C, although the polyp and coenosarc regions of the coral showed no variation across the treatments (Fig. 3f). *P. damicornis* did not show any variation in NPQ with increasing length of exposure to 33°C, and the sign test revealed that the polyp and coenosarc regions did not differ, except for the 33°C/8 h treatment, in which the polyp had a greater NPQ than did the coenosarc (Fig. 3d).

Rapid light curves

The $rETR_{max}$, E_k and Yi for *P. damicornis*, *A. nobilis* and *C. serailia* (Table 1) were determined for each temperature treatment, and separate measurements of the polyps and coenosarc were taken. Measurements of $rETR_{max}$ for *P. damicornis* declined with increasing length of exposure to 33°C. In all but the control treatment, the $rETR_{max}$ of the polyp was greater than that of the coenosarc in the same treatment. The minimum saturating irradiance (E_k) gives an indication of the irradiance at which photochemical utilisation of absorbed quanta transfers to non-photochemical dissipation. In *P. damicornis*, this parameter did not vary over the temperature treatments for either the polyp or the coenosarc. When comparing between polyp and coenosarc structures at each treatment, some significant variation was detected. The Yi values significantly

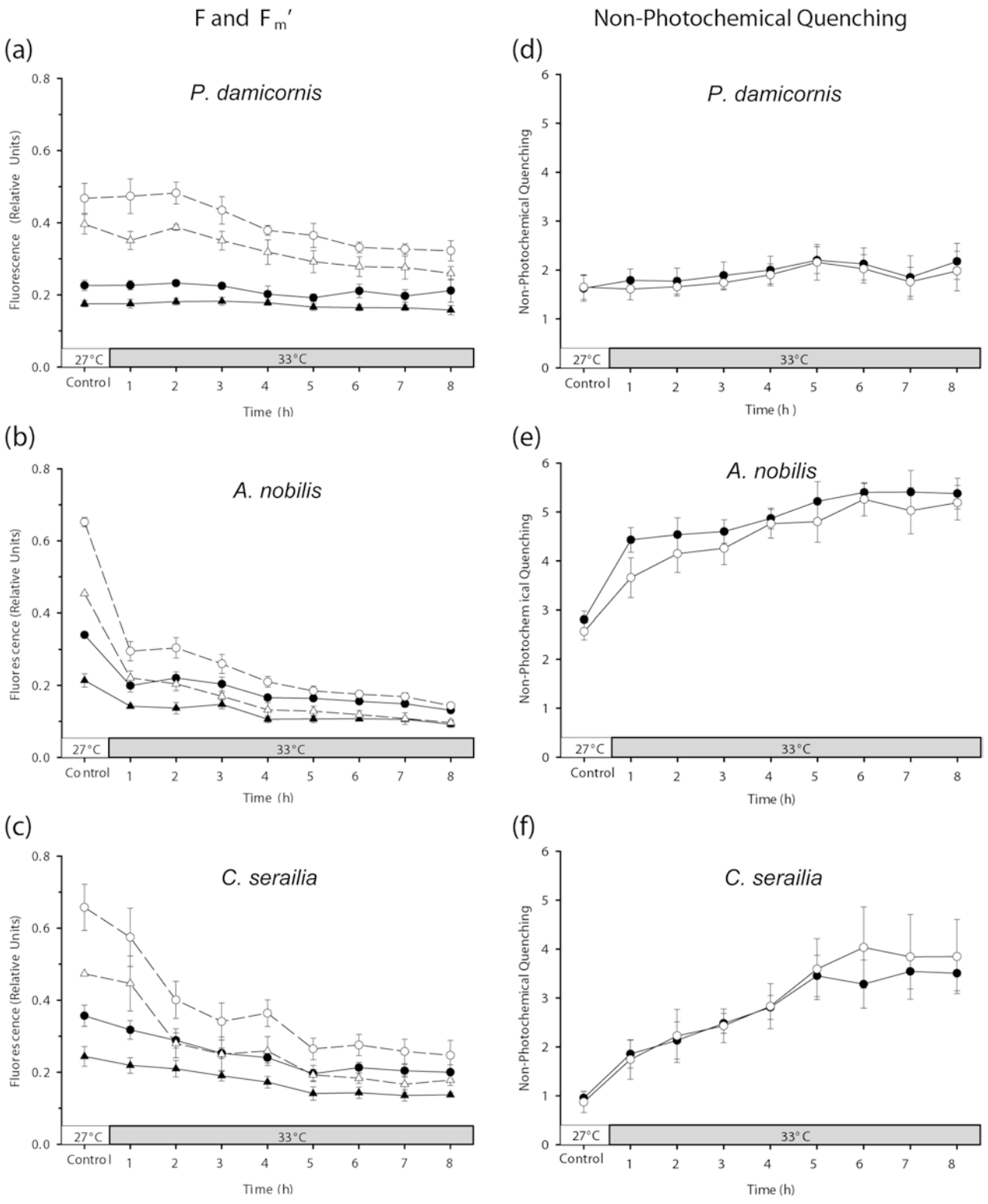

Fig. 3a–f *Pocillopora damicornis*, *Acropora nobilis*, *Cyphastrea serailia*. **a–c** F (*solid lines*, *closed symbols*) and F_m' (*dashed lines*, *open symbols*) of the polyp (*circles*) and coenosarc (*triangles*) showing the control (27°C) and 33°C/0–8 h temperature treatments. **d–f** NPQ of the polyp (*closed circles*) and coenosarc (*open circles*) showing the control (27°C) and 33°C/0–8 h temperature treatments. For all tests, averages (±SE) shown ($n=4$)

declined ($P<0.05$) over the experimental period and the polyp was found to have a higher Φ_{PSII} (Yi) than the coenosarc in all treatments (Table 1).

The $rETR_{max}$, E_k and Yi in *A. nobilis* were found to decline from the control to the 33°C/8 h treatment. The $rETR_{max}$ showed some heterogeneity between the polyp

Table 1 *Pocillopora damicornis*, *Acropora nobilis*, *Cyphastrea serailia*. $rETR_{max}$, E_k and Yi (description of parameters see "Materials and methods") for each temperature treatment. Independent values for the polyp and coenosarc regions are given. Averages (±SE) are shown ($n=4$); significant differences indicated by *asterisk*, where $P<0.05$

Treatment	$rETR_{max}$			E_k			Yi		
	Polyp	Coenosarc	*P*	Polyp	Coenosarc	*P*	Polyp	Coenosarc	*P*
P. damicornis									
27°C	104.0 ± 3.8	99.5 ± 6.5		235.2 ± 11.2	228.4 ± 20.2		0.527 ± 0.03	0.517 ± 0.03	*
33°C/1 h	95.8 ± 5.5	82.4 ± 10.1	*	229.4 ± 7.6	205.4 ± 9.9	*	0.533 ± 0.02	0.507 ± 0.03	*
33°C/2 h	86.3 ± 7.4	76.8 ± 9.2	*	212.0 ± 9.9	148.5 ± 46.4	*	0.514 ± 0.01	0.493 ± 0.01	*
33°C/3 h	86.9 ± 5.5	75.4 ± 5.2	*	218.8 ± 6.3	199.1 ± 7.3	*	0.488 ± 0.01	0.466 ± 0.02	*
33°C/4 h	80.0 ± 6.3	68.8 ± 6.0	*	204.5 ± 10.0	199.2 ± 8.8		0.475 ± 0.01	0.429 ± 0.03	*
33°C/5 h	62.8 ± 2.3	52.7 ± 3.1	*	194.4 ± 23.7	181.4 ± 6.3		0.436 ± 0.02	0.420 ± 0.02	*
33°C/6 h	69.3 ± 6.1	62.5 ± 1.4	*	210.9 ± 20.9	192.8 ± 9.8	*	0.434 ± 0.02	0.400 ± 0.02	*
33°C/7 h	62.3 ± 3.8	55.1 ± 4.3	*	181.7 ± 6.7	181.9 ± 5.6		0.425 ± 0.02	0.399 ± 0.03	*
33°C/8 h	46.6 ± 5.4	54.0 ± 7.3	*	194.7 ± 15.7	183.0 ± 6.2		0.398 ± 0.03	0.364 ± 0.03	*
P-value	0.000*	0.000*		0.212	0.230		0.000*	0.001*	
A. nobilis									
27°C	83.8 ± 4.1	85.6 ± 3.0		199.9 ± 10.3	210.9 ± 9.4		0.469 ± 0.01	0.473 ± 0.01	
33°C/1 h	47.9 ± 4.3	42.6 ± 4.2	*	176.2 ± 5.1	160.9 ± 6.6		0.302 ± 0.02	0.305 ± 0.02	
33°C/2 h	44.7 ± 3.2	44.2 ± 4.3	*	182.0 ± 9.0	160.0 ± 5.5	*	0.316 ± 0.02	0.301 ± 0.03	
33°C/3 h	38.1 ± 5.4	34.3 ± 5.3	*	146.6 ± 12.7	133.7 ± 7.5		0.305 ± 0.03	0.287 ± 0.03	*
33°C/4 h	26.2 ± 2.2	23.0 ± 1.4	*	126.9 ± 3.4	125.4 ± 5.5		0.204 ± 0.02	0.191 ± 0.02	
33°C/5 h	15.6 ± 1.7	11.7 ± 1.5	*	91.9 ± 1.3	82.8 ± 13.8		0.152 ± 0.01	0.152 ± 0.02	
33°C/6 h	8.3 ± 1.4	6.3 ± 0.7	*	60.7 ± 5.8	56.4 ± 3.8		0.093 ± 0.02	0.086 ± 0.03	
33°C/7 h	6.3 ± 0.7	6.0 ± 1.0		48.2 ± 3.3	42.3 ± 4.7	*	0.092 ± 0.01	0.096 ± 0.03	
33°C/8 h	3.2 ± 1.0	4.0 ± 1.5		33.3 ± 5.2	40.2 ± 10.5		0.039 ± 0.02	0.037 ± 0.02	
P-value	0.000*	0.000*		0.000*	0.000*		0.000*	0.000*	
C. serailia									
27°C	127.9 ± 7.9	119.3 ± 6.3	*	335.2 ± 39.2	321.6 ± 42.6		0.456 ± 0.01	0.468 ± 0.02	
33°C/1 h	71.0 ± 7.1	71.2 ± 5.2		269.6 ± 32.6	242.7 ± 26.9	*	0.402 ± 0.02	0.415 ± 0.01	
33°C/2 h	67.3 ± 8.6	85.7 ± 13.0		277.2 ± 38.9	336.0 ± 59.9		0.374 ± 0.01	0.392 ± 0.01	
33°C/3 h	41.9 ± 5.9	43.8 ± 5.3		206.1 ± 17.4	212.6 ± 23.1		0.344 ± 0.03	0.336 ± 0.03	
33°C/4 h	38.3 ± 9.0	35.5 ± 3.7		165.3 ± 26.0	165.9 ± 11.6		0.337 ± 0.02	0.340 ± 0.01	
33°C/5 h	23.7 ± 6.3	20.8 ± 2.8		143.5 ± 26.9	134.0 ± 14.4		0.276 ± 0.04	0.281 ± 0.02	
33°C/6 h	22.8 ± 8.3	17.1 ± 2.7		127.0 ± 35.0	104.8 ± 13.9		0.266 ± 0.03	0.258 ± 0.02	
33°C/7 h	15.1 ± 8.3	12.4 ± 5.4		83.4 ± 26.1	80.4 ± 19.8		0.229 ± 0.05	0.226 ± 0.04	
33°C/8 h	13.2 ± 5.6	10.9 ± 2.9		80.9 ± 19.2	70.7 ± 8.3		0.231 ± 0.05	0.216 ± 0.03	
P-value	0.000*	0.000*		0.000*	0.000*		0.000*	0.000*	

and coenosarc in the 33°C/1–6 h treatments, where the polyp had a greater $rETR_{max}$ than did the coenosarc. For the E_k and Yi parameters there was some heterogeneity found; however, these differences were not consistent over time or temperature.

Finally, *C. serailia* showed a significant decline in $rETR_{max}$, E_k and Yi with increasing length of exposure to 33°C compared to the 27°C control treatment (Table 1). In this species little heterogeneity between the polyp and coenosarc was observed, with only the $rETR_{max}$ being higher in the polyp in the control. E_k was found to the have a higher reading in the polyp in the 33°C/1 h treatment; however, no variation was observed in the Yi values.

Discussion

As demonstrated here, fluorescence imaging is a particularly useful tool for studying the changes in the physiology of corals exposed to bleaching conditions. It has allowed detailed insight into the spatial variation of photosynthesis within a section of a coral colony and has provided further information on the particular areas of the coral structure that are most sensitive to bleaching conditions. In a previous study (Ralph et al. 2002), a Microfibre-PAM and Diving-PAM were used to detect spatial heterogeneity in corals by employing fibre-optic probes of differing tip diameters (8, 1 and 0.14 mm). It was found that coenosarc tissue differed significantly from polyp tissue at a spatial resolution provided by the 1 mm and 0.14 mm fibre probes. The resolution of the Imaging-PAM is 35×36 μm, an intermediate resolution between the 1 mm and 0.14 mm probes. The Imaging-PAM provides a very clear picture of the heterogeneity dictated largely by the distribution of polyps, but showing reduced fluorescence in the tip of a bleached branch.

There are still some unresolved questions about the results from the Imaging-PAM and its ability to accurately relate the photosynthetic properties of coral tissues, which still need to be addressed. These are generally the same as for the Microfibre-PAM (Ralph et al. 2002). Firstly, what part of the population of zooxanthellae is being assessed and does this affect any of the results? The answer will differ between the polyp

and coenosarc tissue. The coenosarc tissue is thinner, and probably most of the zooxanthellae are monitored by the PAM signal. There was little indication of spatial variation within the coenosarc tissue for any fluorescence-derived parameter (Fig. 3). However, it is possible that fine-scale variation may be revealed when an Imaging-PAM with higher pixel resolution becomes available. The polyp tissue is much more complex and has deeper populations of zooxanthellae that are not, or only weakly, monitored by the PAM signal. The zooxanthella populations that are monitored are those in the upper tissue layers, which are adapted to higher light than zooxanthellae in deeper tissue layers. However, given this limitation, it still seems reasonable to compare the outer polyp tissue with the coenosarc tissue, which also harbours high-light-adapted symbionts.

As with the Microfibre-PAM study (Ralph et al. 2002), the present study shows clear differences between the coenosarc and polyp tissue responses (see below). The second concern is whether other photosynthetic components within the coral are also contributing to the response. Since, in the polyps, only some of the zooxanthella populations are assessed and there are no other recorded symbionts in the coral tissue, the real concern is the coenosarc tissue, which is a thin layer over the coral skeleton, which harbours endolithic populations of cyanobacteria and the green alga *Ostreobium*. Cyanobacteria are unlikely to have presented a problem in our study, because the Imaging-PAM used a blue excitation beam, which gives very little signal with cyanobacterial populations (Kolbowski and Schreiber 1995). Moreover, the cyanobacterial populations generally lie nearer to the surface than do the *Ostreobium* green algal populations (Ralph et al., in preparation), thus masking any *Ostreobium* signal.

In comparison with previous studies of micro-heterogeneity in corals (Kühl et al. 1995; Salih et al. 2000; Ralph et al. 2002), the present study clearly shows the advantage of using a fluorescence imaging system like the Imaging-PAM. It allows the quick visualisation of photosynthetic heterogeneity between polyps and coenosarc (Fig. 2), and the identification of spatial gradients of heterogeneity such as those from the tip to more distal regions in some branching corals (Fig. 2). Other spatial differences in photosynthetic performance, such as those from sun-exposed to shaded regions or from raised regions to depressions, should also be possible to visualise in the future. Furthermore, the fact that each field of view has 640×480 pixels for each fluorescence parameter means that subsequent analysis can be based on a much greater number of samples, leading to much better statistical analysis (Fig. 3).

The effect of exposure to 33°C was a continual decline over time of F uniformly across the whole coral structure, as clearly shown in *Acropora nobilis* (Fig. 3b) and *Cyphastrea serailia* (Fig. 3c). The bleaching of zooxanthellae in these two species was thus apparently constant in all regions of the coral and approximately proportional to the time of exposure. Variation along the length of the coral surface imaged was not observed, due to the small size of the area studied (~15 mm^2). The lack of variation in F for *Pocillopora damicornis* across treatments implies that there little bleaching occurred in this species during the experimental period, consistent with previous observations that *P. damicornis* is fairly tolerant of such temperatures (Jones et al. 1998). All species showed similar declines in $rETR_{max}$ with increasing exposure. This has been attributed to an inhibition of the activity of the oxygen-evolving apparatus (Warner et al. 1999), or, alternatively, the inhibition of inorganic carbon acquisition (Jones et al. 1998). A significant drop in F_m' in *A. nobilis* (Fig. 3b) and *C. serailia* (Fig. 3c) with increasing exposure to 33°C showed that the number of active PSII reaction centres was reduced by the onset of the bleaching conditions. A decreasing F_m' also created a greater amount of NPQ, as illustrated in Fig. 3e (*A. nobilis*) and f (*C. serailia*). It seems that, in *A. nobilis* and *C. serailia*, these conditions had an equal impact on the polyp and coenosarc tissue, as F_m' declined at a similar rate in these two tissue types. The sensitivity of the polyp and coenosarc to bleaching, therefore, appear to be quite similar.

In terms of Φ_{PSII} (Fig. 2) and Yi (Table 1), the most sensitive species was *A. nobilis*, which by 8 h at 33°C had reached a Φ_{PSII} of almost zero across its surface. The responses of *P. damicornis* and *C. serailia* were less severe, although a gradual decline in Φ_{PSII} and Yi could still be observed. Heterogeneity in Φ_{PSII} and Yi was found between the polyp and coenosarc tissue in *P. damicornis* (Table 1), where the polyp had a greater Yi for each treatment. It can therefore be concluded that, in this species, although no significant bleaching of zooxanthellae occurred, there were clear stress responses, with different regions responding differently when exposed to bleaching conditions (Table 1). In contrast, *A. nobilis* and *C. serailia* (Table 1) showed very little, if any, heterogeneity in Φ_{PSII} and Yi. The lack of variation in Yi between the two structures leads us to conclude that in these species the different tissue regions respond similarly under bleaching conditions.

The use of the Imaging-PAM to quantify NPQ and to construct rapid light curves from which E_k can be calculated also provides a means to test whether E_k is a useful indicator of the point at which non-photochemical quenching occurs. While the xanthophyll cycle depends on a relatively slow conversion of diadinoxanthin to diatoxanthin in the case of zooxanthellae (Warner et al. 1999), the actual entrainment depends on the ΔpH across the thylakoid membrane, which correlates with the P versus E curve (Gilmore et al. 1998). Furthermore, as corals become more stressed under bleaching conditions, there is an enhanced requirement for dissipation of energy through the xanthophyll cycle if photo-oxidative damage due to the generation of oxygen free radicals is to be reduced. In the case of *A. nobilis* (Fig. 3e) and *C. serailia* (Fig. 3f), prolonged exposure to 33°C did result in an increase in NPQ, whereas *P. damicornis* showed little effect. Also the polyps of

A. nobilis were found to have higher NPQ values compared to the coenosarc tissue in many of the temperature treatments (Fig. 3e). This suggests either: (1) that the zooxanthellae of the polyp require or use NPQ to a greater extent than the surrounding coenosarc regions, or (2) that polyps were more affected by elevated temperatures.

In *A. nobilis* and *C. serailia* E_k declined from about 205 to 37 μmol photons m^{-2} s^{-1} and from 328 to 76 μmol photons m^{-2} s^{-1}, respectively (Table 1), after 8 h at 33°C for polyps and somewhat similarly for coenosarc tissue. The reduction in E_k over time was correlated with an increase in NPQ (Fig. 3e, f; *A. nobilis* $R^2 = 0.802$; *C. serailia* $R^2 = 0.936$), supporting the view that E_k is proportional to the state of non-photochemical quenching (Henley 1993). In *P. damicornis*, however, the lack of change in E_k corroborates Fig. 3d, where NPQ showed no change over time.

In conclusion, the Imaging-PAM clearly showed differential fluorescence patterns between coenosarc and polyp tissues in *P. damicornis* under bleaching conditions. Some further differences between tip and distal regions were revealed in *A. nobilis*. Heterogeneity in the bleaching response could be detected by *F* and NPQ in *A. nobilis* and *C. serailia*; however, in *P. damicornis* Φ_{PSII} and Yi were the most useful parameters for identifying spatial variation. Changes in E_k determined from rapid light curves served as a proxy for changes in NPQ under bleaching conditions in *A. nobilis* and *C. serailia*.

Acknowledgements We thank N. Ralph for the construction of the flow-through chambers and the staff of Heron Island Research Station for support. Specimens were collected under Great Barrier Reef Marine Park Authority permit G01/623. The Australian Research Council, the University of Technology, Sydney, and the University of Sydney provided funding support for A.W.D.L. and P.J.R. The Danish Natural Science Research Council supported M.K. (contract no. 9700549). The experiments comply with the current laws of Australia.

References

Bruno JF, Siddon CE, Witman JD, Colin PL, Toscano MA (2001) El Niño related coral bleaching in Palau, western Caroline Islands. Coral Reefs 20:127–136

Cook CB, Logan A, Ward J, Luckhurst B, Berg CJ (1990) Elevated temperatures and bleaching on a high-latitude coral reef: the Bermuda event. Coral Reefs 9:45–49

Fitt WK, Spero HJ, Halas J, White MW, Porter JW (1993) Recovery of the coral *Montastrea annularis* in the Florida Keys after the 1987 Caribbean 'bleaching event'. Coral Reefs 12:57–64

Fitt WK, Brown BE, Warner ME, Dunne RP (2001) Coral bleaching: interpretation of thermal tolerance limits and thermal thresholds in tropical corals. Coral Reefs 20:51–65

Gilmore AM, Shinkarev VP, Hazlett TL, Govindjee (1998) Quantitative analysis of the effects of intrathylakoid pH and xanthophyll cycle pigments on chlorophyll alpha fluorescence lifetime distributions and intensity in thylakoids. Biochemistry 37:13582–13593

Harrison WG, Platt T (1986) Photosynthesis–Irradiance relationships in polar and temperate phytoplankton populations. Polar Biol 5:153–164

Helmuth BST, Timmerman BEH, Sebens KP (1997) Interplay of host morphology and symbiont microhabitat in coral aggregations. Mar Biol 130:1–10

Henley WJ (1993) Measurement and interpretation of photosynthetic light-response curves in algae in the context of photoinhibition and diel changes. J Phycol 29:729–739

Hoegh-Guldberg O (1999) Climate change, coral bleaching and the future of the world's coral reefs. Mar Freshw Res 50:839–866

Hoegh-Guldberg O, Smith GJ (1989) The effect of sudden changes in temperature, light and salinity on the population density and export of zooxanthellae from the reef *Stylophora pistillata* Esper and *Seriatopora hystrix* Dana. J Exp Mar Biol Ecol 129:279–303

Jones RJ, Hoegh-Guldberg O (1999) Effects of cyanide on coral photosynthesis: implications for identifying the cause of coral bleaching and for assessing the environmental effects of cyanide fishing. Mar Ecol Prog Ser 177:83–91

Jones RJ, Hoegh-Guldberg O, Larkum AWD, Schreiber U (1998) Temperature-induced bleaching of corals begins with impairment of the CO_2 fixation metabolism in zooxanthellae. Plant Cell Environ 21:1219–1230

Kolbowski J, Schreiber U (1995) Computer-controlled phytoplankton analyzer based on 4-wavelengths PAM chlorophyll fluorometer. In: Mathis P (ed) Photosynthesis: from light to biosphere, vol V. Kluwer, Dordrecht, pp 825–828

Kühl M, Revsbech NP (2001) Biogeochemical microsensors for boundary layer studies. In: Boudreau BP, Jørgensen BB (eds) The benthic boundary layer. Oxford University Press, Oxford, pp 180–210

Kühl M, Cohen Y, Dalsgaard T, Barker JB, Revsbech NP (1995) Microenvironment and photosynthesis of zooxanthellae in scleractinian coral studies with microsensors for O_2, pH and light. Mar Ecol Prog Ser 117:159–172

Lewis AE (1966) Biostatistics. Reinhold, New York

Marshall PA, Baird AH (2000) Bleaching of corals on the Great Barrier Reef: differential susceptibilities among taxa. Coral Reefs 19:155–163

Platt T, Gallegos CL, Harrison WG (1980) Photoinhibition of photosynthesis in natural assemblages of marine phytoplankton. J Mar Res 38:687–701

Ralph PJ, Gademann R, Larkum AWD (2001) Zooxanthellae expelled from bleached corals at 33°C are photosynthetically competent. Mar Ecol Prog Ser 220:163–168

Ralph PJ, Gademann R, Larkum AWD, Kühl M (2002) Spatial heterogeneity in active chlorophyll fluorescence and PSII activity of coral tissues. Mar Biol 141:639–646

Ravindran J, Raghukumar C, Raghukumar S (1999) Disease and stress-induced mortality of corals in Indian reefs and observations on bleaching of corals in the Andamans. Curr Sci 76:233–237

Rowan R, Knowlton N (1995) Intraspecific diversity and ecological zonation in coral–algal symbiosis. Proc Natl Acad Sci USA 92:2850–2853

Salih A, Larkum AWD, Cox G, Kühl M, Hoegh-Guldberg O (2000) Fluorescent pigments in corals are photoprotective. Nature 408:850–853

Szmant AM, Gassman NJ (1990) The effects of prolonged bleaching on the tissue biomass and reproduction of the reef coral *Montastrea annularis*. Coral Reefs 8:217–224

Warner ME, Fitt WK, Schmidt GW (1996) The effects of elevated temperature on the photosynthetic efficiency of zooxanthellae in hospite from four different species of reef coral: a novel approach. Plant Cell Environ 19:291–299

Warner ME, Fitt WK, Schmidt GW (1999) Damage to photosystem II in symbiotic dinoflagellates: a determinant of coral bleaching. Proc Natl Acad Sci USA 96:8007–8012

Yentsch CS, Yentsch CM, Cullen JJ, Lapointe B, Phinney DA, Yentsch SW (2002) Sunlight and water transparency: cornerstones in coral research. J Exp Mar Biol Ecol 268:171–183